RESISTANCE TO LTB OF STEEL BRIDGE GIRDERS

Raphaël Thiébaud, Jean-Paul Lebet

École polytechnique fédérale de Lausanne EPFL, School of Architecture,
Civil and Environmental Engineering (ENAC), Steel Structures Laboratory (ICOM), Switzerland
raphael.thiebaud@epfl.ch, jean-paul.lebet@epfl.ch

INTRODUCTION

Lateral torsional buckling (LTB), a complex phenomenon of instability, occurs when a beam is solicited by a bending force. In the area of steel and composite bridges girders which are characterised by slender plate girders, few experimental and theoretical studies exist in order to evaluate their structural security particularly with respect to LTB. Therefore, bridge girder resistance models refer to those existing for beams destined for buildings, by applying nevertheless a high level of conservatism.
Steel bridge girders are three-dimensional structures, the behaviour of which is influenced by a number of parameters such as: cross bracing, variable geometry of cross sections, loading effects or even aspects related to manufacturing and to material. In fact, the manufacturing procedure of plate girders consists of flame cutting and then welding thin web to thick steel sheets. This results in geometric imperfections on the elements as well as in residual stresses inside the material, the effect of which on the behaviour of the structure is not to be neglected. This paper presents the actual results of experimental and theoretical studies carried out on the subject of LTB of steel bridge girders.

1 LTB PARAMETERS AND CODES

The phases of bridge construction that are susceptible to LTB can be summarised in mainly two possible cases: on one hand transitory conditions which correspond to erection phase and on the other hand enduring conditions in operational phase. In comparison with beams destined for buildings, bridge girders feature a number of parameters (cf. *Fig. 1*) which can affect LTB resistance to a greater or a lesser extent.

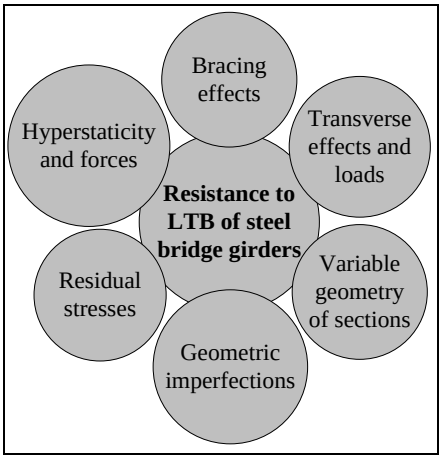

Fig. 1. Parameters affecting LTB resistance of bridge girders

Account is given below on studies conducted in order to determine how important the influence of residual stresses, geometric imperfections and to a lesser extent variable geometry is. Fig. 2 summarizes the conservative state of Eurocode and Swiss code. The corresponding curves of each codes are shown. The most severe reduction curve is the one recommended by EN 1993-2:2006 [1] d curve for Eurocode and then SIA 263:2003 [2] for Swiss code. The estimate of deviation between these extreme values is displayed with the dashed line $\Delta\chi_D$.

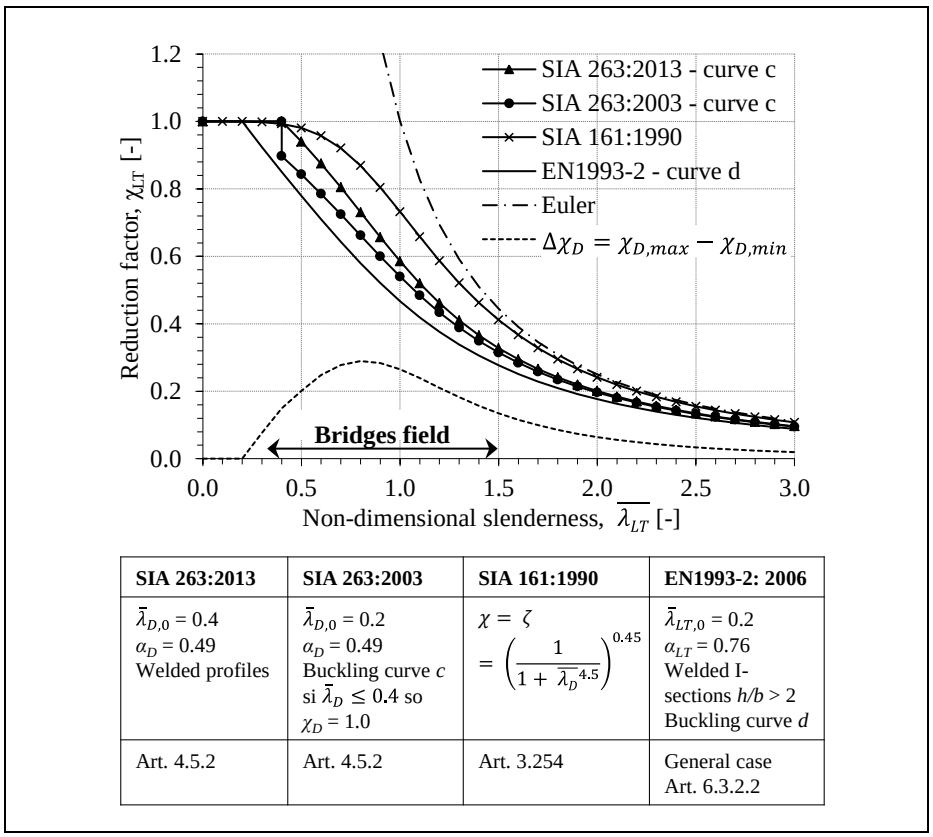

SIA 263:2013	SIA 263:2003	SIA 161:1990	EN1993-2: 2006
$\bar{\lambda}_{D,0}$ = 0.4 α_D = 0.49 Welded profiles	$\bar{\lambda}_{D,0}$ = 0.2 α_D = 0.49 Buckling curve *c* si $\bar{\lambda}_D \leq 0.4$ so χ_D = 1.0	$\chi = \zeta = \left(\frac{1}{1+\bar{\lambda}_D^{4.5}}\right)^{0.45}$	$\bar{\lambda}_{LT,0}$ = 0.2 α_{LT} = 0.76 Welded I-sections *h/b* > 2 Buckling curve *d*
Art. 4.5.2	Art. 4.5.2	Art. 3.254	General case Art. 6.3.2.2

Fig. 2. Representation of different LTB curves on the graph $\chi_D - \overline{\lambda}_{LT}$ or $\overline{\lambda}_D$

The deviation observed is growing until a reduced slenderness of 0.8, then it decreases with an increase in slenderness. It is noteworthy that the largest deviations between curves are in the typical domain of bridge girder slenderness. For example, the difference of reduction coefficients between SIA 161:1990 [3] and l'EN1993-2:2006 can reach 30% for a reduced slenderness of 0.8. For the same slenderness, the difference between SIA 263:2013 [4] and the Eurocode amounts to 15%.

2 EXPERIMENTAL STUDIES

2.1 Measurement of residual stresses

The purpose of these measurements is to define a residual stresses model corresponding to steel bridge girders. Very few models take into consideration all phases of steel bridge girders manufacturing, that is flat rolling, flame cutting of thick flanges and web-flange welding. In what follows, the methology and the main results are presented. The reader may refer to [5] for more details. Measurements constist of two phases. The first phase is dedicated to the study of residual stresses associated to the effect of flame cutting of a steel plate S355N 60mm thick, *Fig. 3a*.

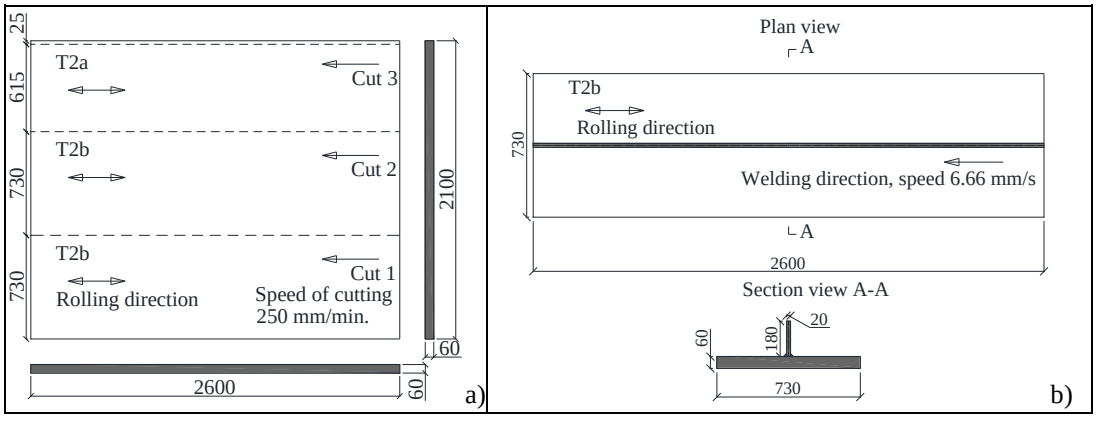

Fig. 3. a) Plan view of flame cutting sequence and b) plan view and cross section of web-flange welding (in mm)

Three successive cuts are performed at a constant velocity of 250 mm/min in order to obtain three flanges. Flanges T1 and T2a are dedicated to the study of residual stresses caused by flame cutting. The second phase, *Fig. 3b*, focuses on the study of welding between a piece of web and the already flame-cut flange T2b. Residual stresses are measured with the sectioning method [6]. Measurement results of residual stresses are presented in *Fig. 4a* for flame-cut samples and in *Fig. 4b* for flame-cut and welded samples.

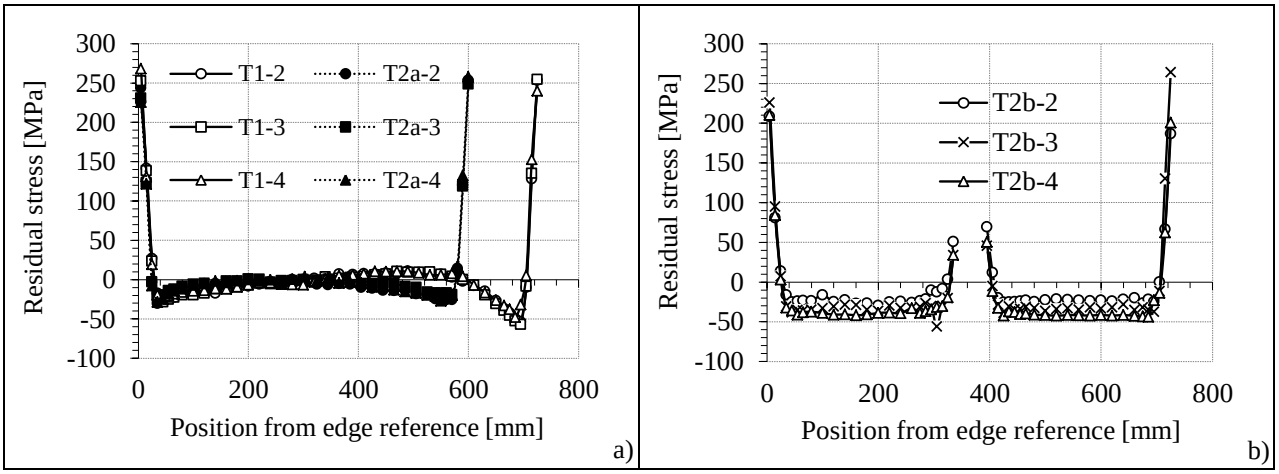

Fig. 4. Distribution of the average residual stresses measured for: a) flame-cut samples (2x3 flame-cut specimen with two different widths: 615 mm and 730 mm) and b) welded samples (1x3 flame-cut and welded specimens)

Fig. 4a shows that flame cutting locally introduces a strong residual tensile stress on edges reaching approximately 250 MPa. This tension component is followed by a compressive zone with a peak of -50 MPa. Stresses are almost zero in the central zone. The effect of the welding of the web to the center of the flange is highlighted in *Fig. 4b*. The main effect of welding is to introduce a tensile stress to the right of the welded zone reaching about 50 MPa at its peak. Therefore, the entire stress distribution is decreased by the same amount normalizing thus the compressive zones to about -30 MPa and lowering the tension peaks to flame-cut edges to 200 MPa. By dividing the edge distance by the sample width b_f and the residual stresses by the yield strength f_y *Fig. 4b* takes a similar form, shown in *Fig. 5a*.

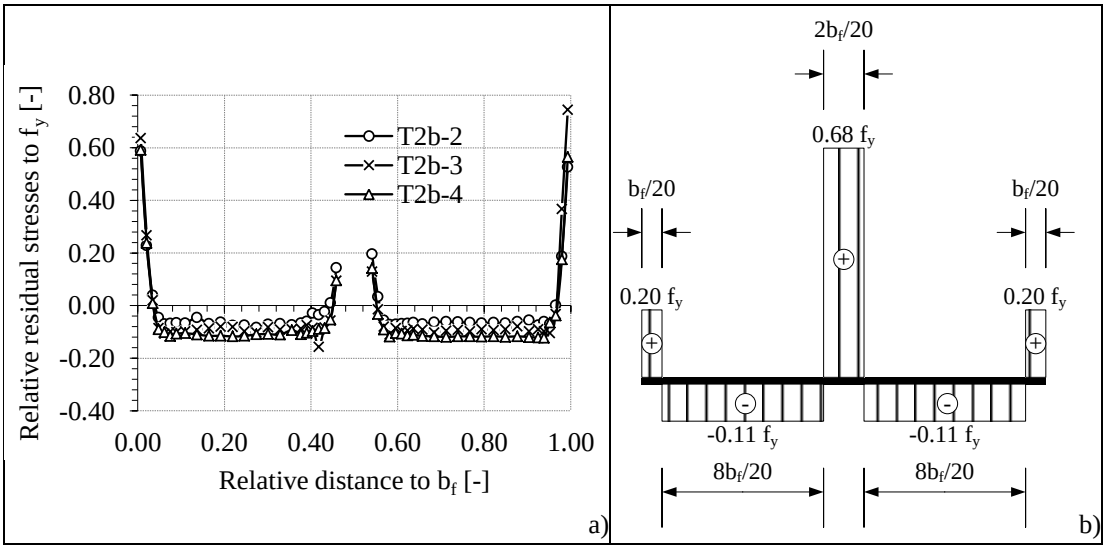

Fig. 5. a) Relative distribution of average residual stresses measured for the welded samples; b) Residual stresses experimental model for a steel plate flame-cut to the edges then welded to the centre.

By successive balancing of the tensile and compressive zones, *Fig. 5a* enables derivation of the experimental model of residual stresses associated to flame cutting and to welding. This model is illustrated in *Fig. 5b.* This model will serve as basis for numerical studies in section 4.

2.2 Measurement of geometric imperfections

The purpose of these measurements is to improve knowledge of geometric imperfections in steel bridge girders. These imperfections are characterized by their shape and their amplitudes, such as global (straightness and curvature) and local (flatness) defects. From a scientific point of view, geometric imperfections should be taken into consideration when calculating the ultimate resistance of a beam. In order to do so, EN 1993-1-5: 2006 annex C [7] suggests a general framework of conservative methods which take into account geometric imperfections for the numerical calculation. Measurements were carried out on two straight steel plate girders used for the construction of the railway viaduct in Wilwisheim, France. One of them corresponds to a suport segment labeled T10 (Fig. 6a) and the other to a span segment labeled T11 (*Fig. 6b*).

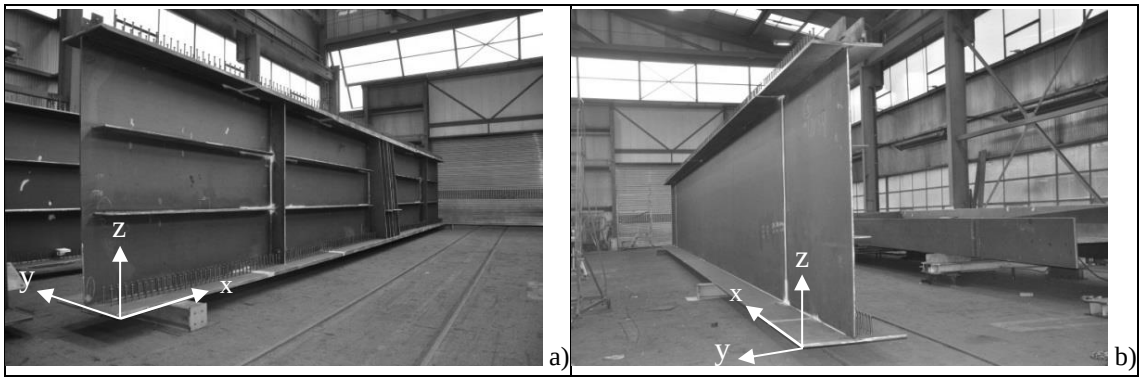

Fig. 6. Measured beams, stocked in laboratory: a) support segment (T10); b) span segment (T11)

The choice of the measurement method is based on a Laser Tracker system sufficiently precise and flexible for industrial work environment. *Fig. 7a* and *b* show measurement results on horizontal straightness. Maximum deviations are compared with the geometric tolerances specified by SIA 263/1:2013 [8] in *Table 1*.

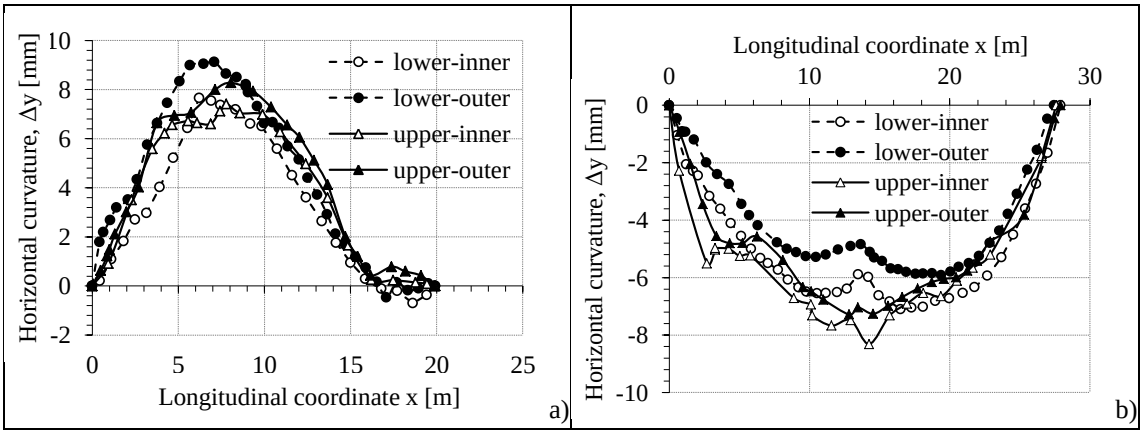

Fig. 7. Measured horizontal (along y) straightness of four edges for each beam, the lower flange (dashed lines) and the upper flange (continuous lines): a) T10, beam support; b) T11, beam span

Table 1. Maximum measured values and tolerance according to SIA 263/1:2013

Beam	Length L [m]	Maximum measured deviation Δy [mm]	Tolerance according to SIA 263/1:2013 $\Delta \leq$ L/1000 [mm]
T10	20	9.1	20
T11	28	8.3	28

In this case, by comparing the maximum measured deviations with the manufacturing and erection tolerances recommended by SIA 263/1:2003, the defects of the measured straightness remain well below the standards. Consequently, it is way on the safe side to take geometric tolerances as geometric imperfection amplitudes, like EN1993-1-5: 2006 suggests when calculating ultimate loading. This result will serve as basis for numerical studies in section 4.

3 NUMERICAL ANALYSIS METHOD

3.1 Finite elements modelling

Numerical models are developped with the non-linear finite elements software FINELG [9]. A typical bridge beam geometry under constant moment and with fork supports is considered. A S355 structural steel is used with its yield strength f_y=355 N/mm^2 following the bi-linear material law.

3.2 Geometric imperfections and residual stresses modeling

In this study the initial imperfection was chosen by considering the geometry of the global mode of buckling analysis which was multiplied either by an amplitude a_1=L/1000 (IG1000 case) or by a_2=L/3000 (IG3000 case) where L is the beam span length. Three schemes of residual stresses, *Fig. 8*, are evaluated. The first case CR0 does not include any residual stresses. The second case CRFCW (*Fig. 8a*) resumes the experimental model developped in section 2.1 which takes into account flange flame cutting and web-flange welding. Residual stresses on the web are taken from [10]. The third model CRW (*Fig. 8b*) takes into account only web-flange welding, ignoring the tension component to flange edges.

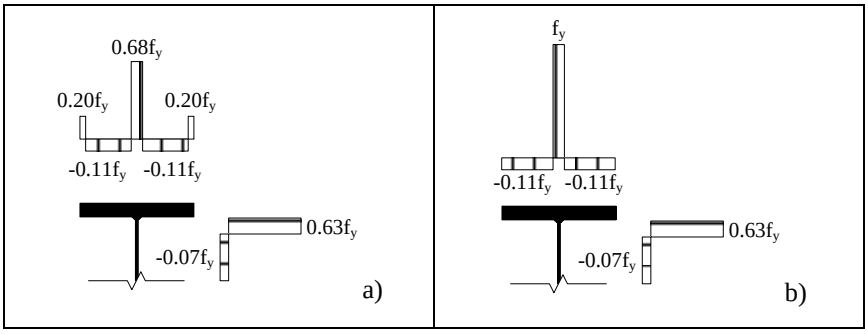

Fig. 8. Schemes of residual stresses under consideration

4 RESULTS OF PARAMETRICAL MODELLING

The parametric study focuses on two typical monosymmetric beam geometries of bridge spans. The calculation method consists of five steps: 1) calculation of LTB critical moment M_{cr} by infinitely elastic linear analysis; 2) non-linear calculation of ultimate moment M_{ult} while integrating geometric and material imperfections; 3) calculation of characteristic moment resistance, sections of class 4, $M_{Rk,EER}$; 4) calculation of reduced slenderness $\bar{\lambda}_D = \sqrt{\frac{M_{Rk,EER}}{M_{cr}}}$; 5) calculation of reduction coefficient $\chi_D = \frac{M_{ult}}{M_{Rk,EER}}$. By varying the beam lengths it is possible to obtain a series of coordinate points $\chi_D - \bar{\lambda}_D$ in order to compare with the different LTB curves.

4.1 Influence of residual stresses, geometric imperfections and geometry

Fig. 9a evaluates residual stresses influence on LTB for beams with St-Pellegrino geometry and geometric imperfection amplitude of L/1000. For reduced slenderness between 0.5 and 1.5, the resulting deviations among the different cases of residual stresses are far from negligible. In this zone, beams without residual stresses (CR0) have the highest rates of resistance. Beams with experimental residual stresses (CRFCW) are more resistant than beams with negligible tension component at the edges (CRW). For a typical reduced slenderness of 0.8, deviations in resistance can reach 5%, (case CRW), 12% (case CRFCW) and 19% (case CR0) compared to SIA 263:2013 – c curve. These deviations are even wider when compared to EN1993-2 - c curve as they reach 20% (case CRW), 27% (case CRFCW) and 34% (case CR0) respectively. The results corresponding to high slenderness, more than $\bar{\lambda}_D = 2.0$, lie above Euler curve. This is explained by two major reasons: 1) the assumption of small rotations according to Euler's theory is no longer respected and 2) the effect of large rotations of beams mobilizes a part of the resistance about the minor axis.

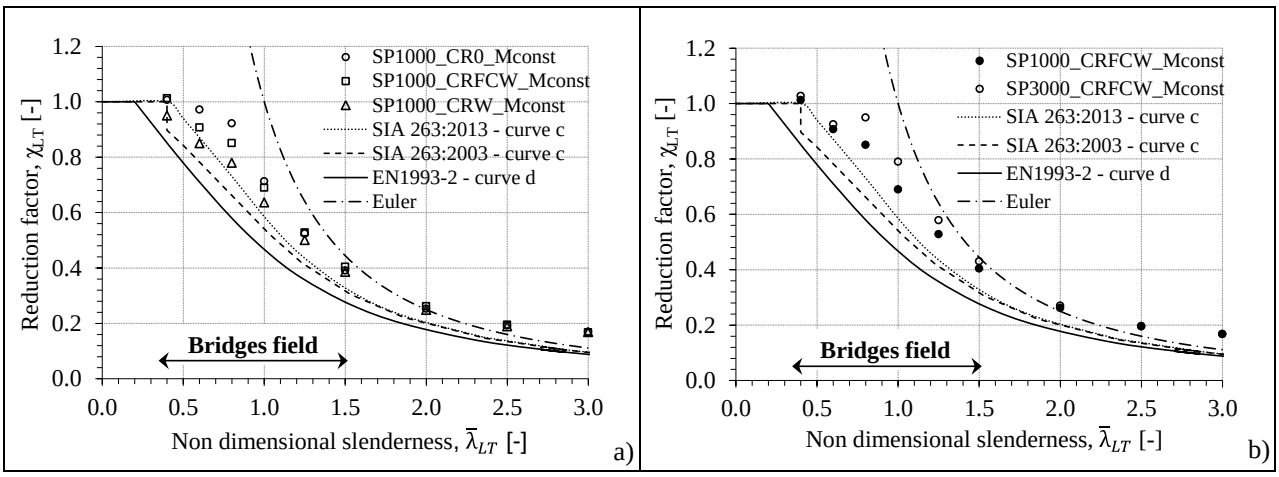

Fig. 9. Influence on LTB of: a) Residual stresses influence, b) geometric imperfections amplitude

Fig. 9b reveals the effect of imperfections amplitude on LTB resistance. Two types of amplitudes are tested; L/1000 recommended by code [7] and L/3000 derived from experimental measurements in section 3.2. Residual stresses measured with CRFCW are used for these two cases. All points lie above LTB curves, sometimes with a significant safety margin. The same trend as in *Fig. 9a* is observed; deviations between the two cases studied are more important in the reduced slenderness zone, which is between 0.5 and 1.5. Generally, when the amplitude of the initial imperfection is lower, case L/3000, the resistance is higher. For $\bar{\lambda}_D = 0.8$, the two cases studied differ up to 10% and the point with imperfection amplitude L/1000 still lies 12% above SIA 263: 2013 curve c. Finally, the effect of the cross section has no particular trend for the geometries considered.

5 CONCLUSION

There are significant differences among reduction curves according to the study of the normative situation for LTB resistance. These differences are particularly important for bridges.
On the one hand, results of experimental studies suggest a residual stress graph adjusted to bridge girders and on the other hand, a more accurate knowledge of geometric imperfections caused by the manufacturing of plate girders. Numerical studies demonstrate the following points:

- effective residual stresses on beam bridge can influence LTB resistance up to 14%
- between cases L/1000 and L/3000, the influence of geometric imperfections amplitude reaches a peak of 10%
- with respect to normative curves, numerical results reveal a significant reserve which should be taken into account (future results of this research)

REFERENCES

[1] EN 1993-2, 2006. *Eurocode 3: Design of steel structures - Part 2: Steel Bridges*, CEN Brussels.
[2] SIA 263, 2003. *Construction en acier*, SIA Zürich.
[3] SIA 161, 1990. *Constructions métalliques*, SIA Zürich.
[4] SIA 263, 2013. *Construction en acier*, SIA Zürich.
[5] Thiébaud, R., Lebet, J.-P., 2012. "Experimental study of residual stresses in thick steel plates", *SSRC Annual Stability Conference Proceedings*, April 17-20, Grapevine, TX, USA.
[6] Tebedge, N., Alpsten, G., Tall, L., 1973. "Residual-stress measurement by the sectioning method". *Experimental Mechanics*, 13(2), pp. 88-96.
[7] EN 1993-1-5, 2006. *Eurocode 3: Design of steel structures - Part 1-5: Plated structural elements*, CEN Brussels.
[8] SIA 263/1, 2013. *Construction en acier – Spécifications complémentaires*, SIA Zürich.
[9] Programme d'élément finis non-linéaire "FINELG", 2003. *User's Manual version 9.0*, Department M & S Université de Liège, Greisch ingénéirie S.A., Liège, Belgium.
[10] Barth, K. E., White, D. W., 1998. "Finite element evaluation of pier moment-rotation characteristics in continuous-span steel I Girders". *Engineering Structures*, 20(8), pp. 761–778.